AD-A051 965 DEFENCE RESEARCH ESTABLISHMENT ATLANTIC DARTMOUTH (NO--ETC F/G 13/10
PREDICTION OF SHIP ROLL, SWAY AND YAW MOTIONS IN OBLIQUE WAVES,(U)
SEP 77 R T SCHMITKE

UNCLASSIFIED DREA-77/4 NL

| OF |
AD
A051 965

END
DATE
FILMED
4-78
DDC

PREDICTION OF SHIP ROLL, SWAY AND YAW MOTIONS IN OBLIQUE WAVES

D.R.E.A. Report 77/4

DEFENCE RESEARCH ESTABLISHMENT ATLANTIC

DARTMOUTH N.S.

D.R.E.A. Report 77/4

PREDICTION OF SHIP ROLL, SWAY AND YAW MOTIONS IN OBLIQUE WAVES

R. T. Schmitke

September 1977

Approved by T. GARRETT Director / Technology Division

DISTRIBUTION APPROVED

R A Kendall

ACTING CHIEF DREA

RESEARCH AND DEVELOPMENT BRANCH
DEPARTMENT OF NATIONAL DEFENCE
CANADA

ABSTRACT

A theoretical model is developed for the prediction of ship lateral motions in oblique seas. The asymptotic behaviour of this model in waves that are long relative to ship beam is examined, with particular emphasis on the classical problem of rolling in beam seas. The theoretical prediction of roll damping is discussed, and the importance of including dynamic lift on appendages is emphasized. Fairly extensive comparisons of predicted and measured roll response are made, with good agreement at all headings considered.

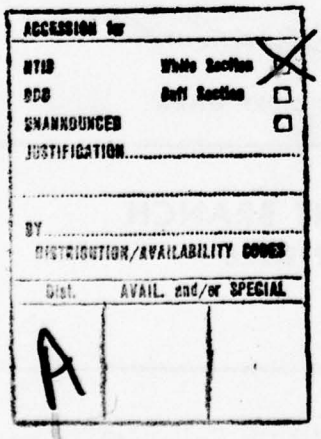

SOMMAIRE

On a mis au point un modéle théorique en vue de prédire les mouvements latéraux de navires dans des mers obliques. On étudie le comportement asymptotique de ce modèle dans des vagues qui sont longues par rapport à la largeur du navire, en mettant l'accent particulièrement sur le problème classique du roulis en mers de travers. On discute de la prédiction théorique de l'amortissement du roulis et on souligne l'importance d'inclure une balancine dynamique sur les appendices. On a comparé un assez grand nombre de résultats en ce qui a trait au roulis prévu et mesuré et on a remarqué un bon niveau de concordance à tous les caps étudiés.

TABLE OF CONTENTS

TABLE OF CONTENTS (CONTD)

NOTATION

A_{jk}	added mass coefficient
B	beam, also damping coefficient
B_{BK}	bilge keel roll damping coefficient
B_E	eddy-making roll damping coefficient
B_F	foil viscous roll damping coefficient
B_H	hull viscous roll damping coefficient
B_{jk}	damping coefficient
C	superscript denoting hull circulation
C_{jk}	restoring coefficient
C_L	lift coefficient
$C_{L\alpha}$	lift curve slope
C_p	prismatic coefficient
C(k)	circulation delay function
C_x	hull cross-section
F	superscript denoting foil contribution
F_j	exciting force or moment
$\overline{GM}$	metacentric height
G(k)	gust function
H	superscript denoting hull contribution
I_4	rolling moment of inertia
I_6	yawing moment of inertia
L	foil lift, also length between perpendiculars
S	foil area
T	draft

U	ship speed
V	superscript for viscous damping
a	wave amplitude
a_{jk}	sectional added mass
a_P	foil added mass
b_{jk}	sectional wave-making damping
b	foil span
b_K	bilge keel breadth
c	foil mean chord
$d\ell$	element of length along girth
f_j	sectional Froude-Kriloff force
g	gravitational acceleration
h	foil mean depth
h_{CG}	height of CG above waterplane
h_j	sectional diffraction force
k	reduced frequency = $.5\omega c/U$
k_w	wave number
m	ship mass
n	roll decay coefficient
n_j	component of unit outward normal to hull
r	distance from bilge keel to CG
s	x-coordinate of foil mid chord
x,y,z	coordinate system
x_p	x-coordinate of centre of area of hull underwater profile
Γ	foil dihedral angle

α	foil angle of attack
β_s	heading angle relative to sea direction
$\overline{\zeta}$	wave slope
η_2	sway displacement
η_4	roll angle
η_6	yaw angle
ξ	variable of integration in longitudinal direction
ρ	water density
ϕ_j	two-dimensional section potential
ω	frequency of encounter
ω_w	wave frequency

1. INTRODUCTION

Over the past two decades, considerable success has been achieved in the theoretical prediction of ship heave and pitch motions. Computer programs to perform such predictions are now in common use, and a large number of correlation studies have shown that the accuracy of the absolute motion predictions is generally very satisfactory. For lateral plane motions, however, of which by far the most important is roll, the situation is much different. Although several programs exist which predict roll, sway and yaw by purely theoretical means, for example Reference 1, correlation studies[2] have shown that errors in roll prediction are generally significant, particularly for high speed warship hull forms. As to sway and yaw, correlation studies have been very few and inconclusive.

The fundamental reason for the discrepancies reported in correlation studies is that programs such as Reference 1 generally make inaccurate estimates of roll damping, especially at higher speeds. Experience with these programs has led to the widely held belief that the roll damping prediction problem is so complex and non-linear as to be theoretically intractable. In keeping with this philosophy, certain computer programs[3] require that the roll damping coefficient be input by the user. Model test programs specifically dedicated to the experimental determination of roll damping are fairly common.

The failure of Reference 1 to make accurate predictions of roll damping may be traced to an inadequate treatment of hull appendages, and in particular to the failure to include the effects of dynamic lift on such appendages as rudders, skegs and propeller shaft brackets. The theory presented in this report includes these effects and consequently produces good estimates of both roll damping and roll response. Demonstration of a conceptually simple yet reliable technique for roll damping prediction is probably the single most important contribution of the present report.

The theory presented herein has basically four facets:

1) Strip theory for computing hull added mass, wavemaking damping and exciting forces.

2) Lifting surface contributions to damping and exciting forces.

3) Viscous roll damping, principally from bilge keels.

4) Hull circulatory effects.

After a detailed presentation of theory, asymptotic expressions valid for long waves are derived and discussed in order to provide a physical "feel" for the mathematical model. Roll damping is then discussed and examples are presented showing the relative significance of the various contributions to roll damping. Finally, theoretical predictions are compared with experimental data, principally from regular wave tests of a fully-appended self-propelled frigate model. Agreement is generally good and it is concluded the theory yields results of sufficient accuracy for preliminary design purposes.

2. EQUATIONS OF MOTION

In applying strip theory to a displacement hull, certain assumptions are standard:

i) Ship response is a linear function of wave excitation.

ii) Ship length is much greater than either beam or draft.

iii) All viscous effects other than roll damping are negligible.

iv) The hull does not develop appreciable planing lift.

The linear equations of motion for the ship without roll stabilizers are given below. These are written with respect to a stability axis system fixed in the ship; this axis system is slightly different from the translating earth axes employed in Reference 4. Stability axes are commonly used in dynamic simulation of both aircraft and marine vehicles. In the present case, stability axes offer the advantage of being more suitable for control studies and of yielding simpler expressions for the coefficients of the equations of motion. Further, hull circulatory effects are included in the mathematical model, and expressions given in the literature for these effects are written in terms of stability axes. The axis system is illustrated in Figure 1. The axes are fixed in the ship with origin at the CG, and in the reference con-

dition of steady forward speed with no seaway or control disturbances, the x-axis is directed horizontally forward, the z-axis vertically upward, and the y-axis to port.

The coupled sway, roll and yaw equations follow, with notation the same as in Reference 4.

$$\text{Sway:}\quad (A_{22} + m)\ddot{\eta}_2 + B_{22}\dot{\eta}_2 + A_{24}\ddot{\eta}_4 + B_{24}\dot{\eta}_4 + A_{26}\ddot{\eta}_6 + (B_{26} + mU)\dot{\eta}_6 = F_2 \quad (1)$$

$$\text{Roll:}\quad A_{24}\ddot{\eta}_2 + B_{24}\dot{\eta}_2 + (A_{44} + I_4)\ddot{\eta}_4 + B_{44}\dot{\eta}_4 + C_{44}\eta_4 + A_{46}\ddot{\eta}_6 + B_{46}\dot{\eta}_6 = F_4 \quad (2)$$

$$\text{Yaw:}\quad A_{62}\ddot{\eta}_2 + B_{62}\dot{\eta}_2 + A_{64}\ddot{\eta}_4 + B_{64}\dot{\eta}_4 + (A_{66} + I_6)\ddot{\eta}_6 + B_{66}\dot{\eta}_6 = F_6 \quad (3)$$

where η_2 is sway, η_4 roll and η_6 yaw. A_{jk} and B_{jk} are the added mass and damping coefficients, C_{jk} are the restoring coefficients, and F_j are the exciting forces and moments. These coefficients are ascribed the general forms:

$$A_{ij} = A^H_{ij} + A^F_{ij} \quad (4)$$

$$B_{ij} = B^H_{ij} + B^F_{ij} + B^C_{ij} \quad (5)$$

$$F_i = F^H_i + F^F_i + F^C_i \quad (6)$$

where superscript H denotes hull coefficients derived from strip theory, superscript F signifies contributions due to appendages (foils) such as rudders and fins, and superscript C denotes hull circulatory terms.

For B_{44}, the roll damping coefficient, there is an additional term, B^{V}_{44}, the viscous roll damping coefficient. This takes account of the viscous resistance to rolling of bilge keels, skeg, hull, rudder and other appendages.

Detailed expressions for the terms on the right hand side of equations (4) to (6) are given in Sections 3 to 5.

3. HULL COEFFICIENTS DERIVED FROM STRIP THEORY

The strip theory from which the hull coefficients are derived is given in Reference 5.

3.1 ADDED MASS AND WAVE-MAKING DAMPING

The expressions given below for hull added mass and damping are considerably simpler than the corresponding expressions in Reference 5. This results from using stability axes instead of translating earth axes. The transformations involved are discussed in Appendix A.

$$A^{H}_{22} = \int_{L} a_{22} d\xi \tag{7}$$

$$B^{H}_{22} = \int_{L} b_{22} d\xi \tag{8}$$

$$A^{H}_{24} = \int_{L} a_{24} d\xi \tag{9}$$

$$B^{H}_{24} = \int_{L} b_{24} d\xi \tag{10}$$

$$A^{H}_{26} = \int_{L} a_{22} \xi d\xi \tag{11}$$

$$B_{26}^{H} = \int_{L} b_{22} \xi d\xi \tag{12}$$

$$A_{44}^{H} = \int_{L} a_{44} d\xi \tag{13}$$

$$B_{44}^{H} = \int_{L} b_{44} d\xi \tag{14}$$

$$A_{46}^{H} = \int_{L} a_{24} \xi d\xi \tag{15}$$

$$B_{46}^{H} = \int_{L} b_{24} \xi d\xi \tag{16}$$

$$A_{62}^{H} = A_{26}^{H} - UB_{22}^{H}/\omega^2 \tag{17}$$

$$B_{62}^{H} = B_{26}^{H} + UA_{22}^{H} \tag{18}$$

$$A_{64}^{H} = A_{46}^{H} - UB_{24}^{H}/\omega^2 \tag{19}$$

$$B_{64}^{H} = B_{46}^{H} + UA_{24}^{H} \tag{20}$$

$$A_{66}^{H} = \int_{L} a_{22} \xi^2 d\xi \tag{21}$$

$$B_{66}^{H} = \int_{L} b_{22} \xi^2 d\xi \tag{22}$$

The above integrations are over the length of the ship. In practice, the hull length is divided into approximately 20 sections and the two-dimensional added mass (a_{jk}) and wave-making damping (b_{jk}) are computed for each section. a_{22} and

b_{22} result from swaying motions, a_{44} and b_{44} apply to roll, while a_{24} and b_{24} are due to cross-coupling between sway and roll.

3.2 HYDROSTATIC RESTORING COEFFICIENT

The only hydrostatic restoring coefficient affecting lateral motions is C_{44}:

$$C_{44} = mg\overline{GM} \tag{23}$$

where $\overline{GM}$ is metacentric height.

3.3 FORCING FUNCTIONS

The strip theory of Reference 5 yields the following expressions for the sway exciting force F_2^H, the roll exciting moment F_4^H, and the yaw exciting moment F_6^H.

$$F_j^H = \rho a \int_L (f_j + h_j) d\xi \qquad j = 2, 4 \tag{24}$$

$$F_6^H = \rho a \int_L [(f_2 + h_2)\xi + \frac{U}{i\omega} h_2] d\xi \tag{25}$$

where a is the amplitude of the incident wave and the integration is over the hull length. f_j and h_j are the sectional incident and diffraction forces, respectively, given by

$$f_j(x) = -g \exp(-ik_w x \cos\beta_s) \int_{C_x} n_j \exp(ik_w y \sin\beta_s + k_w z') d\ell \tag{26}$$

$$h_j(x) = \omega_w \exp(-ik_w x \cos\beta_s) \int_{C_x} \phi_j (in_3 - n_2 \sin\beta_s) \exp(ik_w y \sin\beta_s + k_w z') d\ell \tag{27}$$

f_j is also commonly referred to as the Froude-Kriloff force. A physical interpretation of f_j and h_j is that f_j results directly from the action of the incident wave system on the hull, while h_j represents a correction for ship-wave interference (diffraction). The integrations are performed over the submerged hull section C_x. n_2 and n_3 are the y and z components of the unit outward normal to the hull at (x, y, z), Figure 1, and

$$n_4 = yn_3 - zn_2 \tag{28}$$

$$z' = z + h_{CG} \tag{29}$$

ϕ_2 and ϕ_4 are the two-dimensional section potentials for sway and roll oscillations. ω_w is wave frequency and k_w is wave number, given by

$$k_w = \frac{\omega_w^2}{g} \tag{30}$$

h_{CG} is the height of the centre of gravity above the waterplane, and β_s is the heading angle relative to the sea, defined in Figure 2. Note that for head seas $\beta_s = 180^o$, for beam seas $\beta_s = 90^o$, and for following seas $\beta_s = 0^o$. ω_w is related to ω, the frequency of encounter, by

$$\omega = \omega_w - k_w U \cos\beta_s \tag{31}$$

4. VISCOUS ROLL DAMPING

The viscous roll damping coefficient may be expressed as follows:

$$B_{44}^{V} = B_{BK} + B_{E} + B_{H} + B_{F} \tag{32}$$

where B_{BK}, B_{E} and B_{H} denote contributions from bilge keels, eddy-making resistance of the hull and hull friction, respectively. B_{F} represents the viscous effect of appendages other than bilge keels (rudders, fins, etc.) at zero speed. Of the four components of B_{44}^{V}, B_{BK} is normally by far the largest.

Viscous roll damping is, of course, a non-linear function of roll amplitude. A linear approximation is obtained by equating the energy dissipated by the non-linear viscous effect during one roll cycle to that dissipated by a linear damping term. This is done as follows:

Denote by B the linear damping coefficient and let the roll angle be given by

$$\eta_4 = \hat{\eta}_4 \sin\omega t \tag{33}$$

where $\hat{\eta}_4$ is the roll amplitude. Now $B\dot{\eta}_4$ represents a torque about the CG and during one roll cycle the following amount of work must be done against this torque:

$$4\int_0^{\hat{\eta}_4} B\dot{\eta}_4 d\eta_4 = 4\omega^2 B\int_0^{\pi/2\omega} \cos^2\omega t \, dt = \pi\omega B\hat{\eta}_4^2 \tag{34}$$

If the energy dissipated by the viscous effect is E, then B is given by

$$B = \frac{E}{\pi\omega\hat{\eta}_4^2} \tag{35}$$

4.1 BILGE KEELS

The most complete study to date of the effect of bilge keels on ship rolling has been carried out by Kato[6], who found that the following factors influenced bilge keel effectivness: bilge keel area, breadth and aspect ratio, Reynolds number,

ship draught, distance from the bilge keel to the CG, height of the CG and form of the bilge. After analyzing considerable experimental data, he devised the following empirical method for calculating the energy dissipated through bilge keel action.

The energy dissipated in one roll cycle is given by

$$E = 4\rho \ell b_k r \hat{\eta}_4 \left[\frac{r\hat{\eta}_4}{T}\right]^2 C_o C_a C_k C_n \text{Ⓑ} F^{-\alpha} \tag{36}$$

where ℓ is the bilge keel length, b_k bilge keel breadth, r the distance from the center of the bilge keel to the CG and T is the period. C_o, C_a, C_k, C_n, B and F are coefficients depending on ship form and Reynolds number.

A close look at equation (36) shows that a viscous force of the usual form,

$$F_V = \frac{1}{2}\rho V_R^2 S_{BK} C_{BK} \tag{37}$$

acts on the bilge keel with moment arm r about the CG. V_R is average velocity of the bilge keel due to roll, S_{BK} is bilge keel area and C_{BK} is a drag coefficient. Equations to compute the various components of C_{BK} (C_o, C_a, etc.) are given in Appendix B.

From equations (35) and (36), the bilge keel damping coefficient is given by

$$B_{BK} = \frac{1}{\pi^3}\rho \ell b_k r^3 \omega \hat{\eta}_4 C_o C_a C_k C_n \text{Ⓑ} F^{-\alpha} \tag{38}$$

In evaluating B_{BK} the same approach is taken as in computing added-mass and wave-making damping, i.e., the

sectional contributions are computed individually and then summed.

4.2 EDDY-MAKING

The results of this section are due to Tanaka[7], who conducted rolling experiments with various ship sections to assess the effect of section shape on eddy-making roll damping.

The roll-resisting force due to eddy-making is expressed as

$$F = \frac{1}{2}\rho(r\dot{\eta}_4)^2 SC \tag{39}$$

where r is the distance from the CG to the point on the hull where the eddies are generated, S is wetted surface area of the hull section, and C is a drag coefficient depending on hull form.

Now F exerts a torque about the CG given by

$$T = Fr = \frac{1}{2}\rho r^3 SC\hat{\eta}_4^2\omega^2\cos^2\omega t \tag{40}$$

The energy dissipated by this torque during one roll cycle is

$$E = 4\int_0^{\hat{\eta}_4} T d\eta_4 = \frac{4}{3}\rho r^3\hat{\eta}_4^3\omega^2 SC \tag{41}$$

whence, from (35), the eddy-making damping coefficient is

$$B_E = \frac{4}{3\pi}\rho\omega\hat{\eta}_4 r^3 SC \tag{42}$$

It remains to evaluate C. Empirical expressions for

C as a function of section shape are given in Appendix C.

4.3 HULL FRICTION

In Appendix D it is shown that the hull frictional damping coefficient is given by

$$B_H = \frac{4}{3\pi}\rho\omega\hat{\eta}_4 C_{DF}\int_L dx\int_{C_x} r(y\eta_2 + z\eta_3)^2 d\ell \qquad (43)$$

where C_{DF} is the skin friction drag coefficient, C_x is a hull cross-section, $d\ell$ is a girth-wise length element and

$$r = (y^2 + z^2)^{1/2} \qquad (44)$$

If forward speed U is non-zero, the Schoenherr line based on smooth turbulent flow is used to evaluate C_{DF}:

$$C_{DF} = .0004 + (3.46\ \log(\frac{UL}{\nu}) - 5.6)^{-2} \qquad (45)$$

where .0004 is the standard roughness correction and ν is kinematic viscosity. Note that the Reynolds number is based on forward speed, U, and the length between perpendiculars, L.

If U = 0, C_{DF} is evaluated by the following method, due to Kato[8].

$$C_{DF} = 1.328R_n^{-.5} + .014R_n^{-.114} \qquad (46)$$

$$R_n = \frac{3.22}{T\nu}(\overline{r}\hat{\eta})^2 \qquad (47)$$

$$\bar{r} = \frac{1}{\pi}\{(.887 + .145C_B)(1.7T + BC_B) + 2(\overline{KG} - T)\} \qquad (48)$$

where C_B is the block coefficient, $\overline{KG}$ height of the CG above the keel, B ship beam and T draft. R_n is a Reynolds number based on average rolling velocity and average distance from the CG, $\bar{r}$.

4.4 APPENDAGES OTHER THAN BILGE KEELS

At zero forward speed, viscous drag forces opposing roll act on appendages such as rudders and fins. By regarding these as oscillating flat plates and applying the method described by equations (33) to (35), we obtain the following expression for the appendage viscous roll damping coefficient:

$$B_F = \frac{4}{3\pi}\rho\omega\hat{\eta}_4 \Sigma(y^2 + z^2)^{3/2} SC_n \qquad (49)$$

where summation is over all foil elements. C_n is the normal-force coefficient for a flat plate inclined at a large angle to the flow; Hoerner[9] gives a value of 1.17 for C_n when the angle of inclination exceeds 40^o.

5. LIFTING SURFACE CONTRIBUTIONS

When U > 0, hull appendages such as the rudder, skeg and propeller shaft brackets act as lifting surfaces to generate both damping and exciting forces; the contribution to roll damping is especially significant. Of lesser importance are the appendage added mass terms, which are independent of speed.

Since derivation of the lifting surface (foil) coefficients is adequately described in Reference 4, only the final results will be presented herein. Expressions for the foil added mass and damping coefficients are:

$$A^F_{22} = \Sigma a_p \sin^2\Gamma \tag{50}$$

$$B^F_{22} = \frac{1}{2}\rho U \Sigma S C_{L\alpha} C(k) \sin^2\Gamma \tag{51}$$

$$A^F_{24} = -\Sigma a_p \sin\Gamma (y \cos\Gamma + z \sin\Gamma) \tag{52}$$

$$B^F_{24} = -\frac{1}{2}\rho U \Sigma S C_{L\alpha} C(k) \sin\Gamma (y \cos\Gamma + z \sin\Gamma) \tag{53}$$

$$A^F_{26} = \Sigma a_p s \sin^2\Gamma = A^F_{62} \tag{54}$$

$$B^F_{26} = \frac{1}{2}\rho U \Sigma S C_{L\alpha} C(k)(s - c/4)\sin^2\Gamma \tag{55}$$

$$A^F_{44} = \Sigma a_p (y \cos\Gamma + z \sin\Gamma)^2 \tag{56}$$

$$B^F_{44} = \frac{1}{2}\rho U \Sigma S C_{L\alpha} C(k)(y \cos\Gamma + z \sin\Gamma)^2 \tag{57}$$

$$A^F_{46} = -\Sigma a_p s \sin\Gamma (y \cos\Gamma + z \sin\Gamma) \tag{58}$$

$$B^F_{46} = -\frac{1}{2}\rho U \Sigma S C_{L\alpha} C(k) \sin\Gamma (s - c/4)(y \cos\Gamma + z \sin\Gamma) \tag{59}$$

$$B^F_{62} = \frac{1}{2}\rho U \Sigma x S C_{L\alpha} C(k) \sin^2\Gamma \tag{60}$$

$$B^F_{64} = -\frac{1}{2}\rho U \Sigma x S C_{L\alpha} C(k) \sin\Gamma (y \cos\Gamma + z \sin\Gamma) \tag{61}$$

$$A_{66}^{F} = \Sigma a_p s^2 \sin^2\Gamma \tag{62}$$

$$B_{66}^{F} = \frac{1}{2}\rho U \Sigma S C_{L\alpha} C(k)(s - c/4)x \sin^2\Gamma \tag{63}$$

Summation is over all foil elements, including rudder, skeg, fins and propeller shaft brackets. In applying these expressions to the rudder and skeg, the dihedral angle Γ for fins and brackets is illustrated in Figure 3. a_p is the added mass of a foil being accelerated perpendicular to its surface. For sufficiently large aspect ratios, such as the A-brackets,

$$a_p = \pi\rho b(\frac{c}{2})^2 \tag{64}$$

For very low and low aspect ratio foils, such as the skeg and rudder, use empirical expressions for a_p.

A small additional contribution to B_{44} is obtained by regarding the bilge keels as very low aspect ratio lifting surfaces:

$$B_{BK} = \pi\rho U b_k^2 r^2 \tag{65}$$

where b_k is bilge keel breadth and r the distance from bilge keel to the CG.

The exciting forces acting on the appendages are obtained by modifying the foil exciting forces in Reference 4 to apply to arbitrary directions to the sea.

$$F_2^F = \Sigma f_2^F \sin\Gamma \tag{66}$$

$$F_4^F = -\Sigma f_2^F (y \cos\Gamma + z \sin\Gamma) \tag{67}$$

$$F_6^F = \Sigma f_2^F s \sin\Gamma \tag{68}$$

where f_2^F is the sway exciting force acting on an individual foil element:

$$f_2^F = -\omega_w(\sin\Gamma\sin\beta_s + i\cos\Gamma)(\tfrac{1}{2}\rho U S C_{L\alpha} G(k) + i\omega a_p)$$

$$\exp[-k_w(h + i(x\cos\beta_s - y\sin\beta_s))] \tag{69}$$

The methods given in Reference 10 are used to evaluate C(k), the circulation delay function, and G(k), a modified form of Jones' gust function. k is the reduced frequency. a_p is foil added mass and is included in equation (69) to account for the effect of wave orbital acceleration.

6. HULL CIRCULATORY EFFECTS

Consider now the hull circulatory terms. These are evaluated following the methods given in Reference 11. Let

$$B_C = \tfrac{\pi}{2}\rho U T^2 \tag{70}$$

where T is draft. Then, from Reference 11,

$$B_{22}^C = B_C \tag{71}$$

$$B_{26}^C = B_C x_p = B_{62}^C \tag{72}$$

$$B_{66}^C = B_C(\tfrac{1}{2}C_p L)^2 + U\int_L a_{22}\xi d\xi \tag{73}$$

where x_p is the x-coordinate of the centre of area of the hull underwater profile and C_p is the prismatic coefficient.

The action on the hull of the horizontal component of wave orbital velocity generates contributions to the sway and yaw exciting forces. These are estimated by assuming that the hull is a wing with chord L and span varying with sectional draft, and further that lift is uniformly distributed along the ship's length. The resulting terms are given below:

$$f_2^C = \omega_w T_x \sin\beta_s \exp[-k_w(ix\cos\beta_s + T_x/2)] \tag{74}$$

$$F_2^C = -\frac{B_C}{S_p}\int_L f_2^C dx \tag{75}$$

$$F_6^C = -\frac{B_C}{S_p}\int_L f_2^C x\, dx \tag{76}$$

7. LATERAL MOTIONS IN LONG WAVES

It is difficult to obtain from the foregoing mathematics a physical appreciation of the theoretical model; in particular, the expressions for the hull exciting forces are rather abstract in appearance. However, when wavelengths are long compared with the ship's beam, fairly simple approximations may be derived for the hull forcing functions. These asymptotic expressions provide the basis for further theoretical analysis of the lateral motion problem. This study leads to instructive insight into the relative significance of the various terms in the equations of motion, particularly for the classical beam sea problem.

7.1 ASYMPTOTIC BEHAVIOUR OF THE HULL FORCING FUNCTIONS

Asymptotic expressions valid for waves long relative to ship beam will now be derived for the hull forcing functions. Consider first the sectional wave incident force,

equation (26), and expand the complex exponential in the integral to give

$$I = \int_{C_x} n_j \exp(k_w z')(\cos p + i \sin p) d\ell \tag{77}$$

where, for convenience,

$$p = k_x y \sin\beta_s \tag{78}$$

From symmetry considerations, the $n_j \cos p$ term integrates to zero for $j = 2, 4$, since n_j (port) $= -n_j$ (starboard). Hence

$$I = i\int_{C_x} n_j \exp(k_w z') \sin p \, d\ell \tag{79}$$

Now, when wavelength is long relative to beam,

$$\sin p = p, \quad \exp(k_w z') = 1 \tag{80}$$

and the following approximation is obtained

$$I = ik_w \sin\beta_s \int_{C_x} n_j y d\ell \tag{81}$$

Now, for $j = 2$, since $n_2 = dz/d\ell$

$$I = ik_w \sin\beta_s \int_{C_x} y dz = ik_w \sin\beta_s A_x \tag{82}$$

where A_x is sectional area.

For $j = 4$, from equation (28),

$$I = ik_w \sin\beta_s \int_{C_x} (yn_3 - zn_2) y d\ell = -ik_w \sin\beta_s M_x \tag{83}$$

where M_x is the sectional contribution to the roll-restoring moment (see Appendix E).

Combining equations (26), (81) and (83) yields the following long wave approximations for the sectional incident force:

$$f_2 = -ik_w g \sin\beta_s A_x \exp(-ik_w x \cos\beta_s) \tag{84}$$

$$f_4 = ik_w g \sin\beta_s M_x \exp(-ik_w x \cos\beta_s) \tag{85}$$

Consider next the sectional diffraction force, equation (27), and expand the complex exponential in the integral.

$$\begin{aligned} I &= \int_{C_x} \phi_j \exp(k_w z')(in_3 - n_2 \sin\beta_s)(\cos p + i \sin p) d\ell \\ &= \int_{C_x} \phi_j \exp(k_w z')[i(n_3 \cos p - n_2 \sin\beta_s \sin p) \\ &\quad - n_3 \sin p - n_2 \sin\beta_s \cos p] d\ell \end{aligned} \tag{86}$$

From symmetry considerations, the term in brackets multiplying i integrates to zero for $j = 2, 4$, since

$$\phi_j \text{ (port)} = -\phi_j \text{ (starboard)} \quad \text{for } j = 2, 4$$

$$n_2 \text{ (port)} = -n_2 \text{ (starboard)}$$

$$\sin p \text{ (port)} = -\sin p \text{ (starboard)}$$

Hence,

$$I = -\int_{C_x} \phi_j \exp(k_w z')(n_3 \sin p + n_2 \sin\beta_s \cos p)\, d\ell \tag{87}$$

In long waves, the approximations (80) apply, as well as

$$\cos p = 1 \tag{88}$$

$$\therefore I = -\int_{C_x} \phi_j (n_3 k_w y \sin\beta_s + n_2 \sin\beta_s)\, d\ell$$

$$= -\sin\beta_s \int_{C_x} \phi_j n_2 \, d\ell \tag{89}$$

since k_w is small.

By definition[5],

$$\int_{C_x} \phi_j n_2 \, d\ell = \frac{i}{\rho\omega}(\omega^2 a_{2j} - i\omega b_{2j}) \tag{90}$$

Combining (27) and (90) yields the following long wave approximation for the sectional diffraction force:

$$h_j = \frac{-\omega}{\rho} \sin\beta_s (b_{2j} + i\omega a_{2j}) \exp(-ik_w x \cos\beta_s) \tag{91}$$

7.2 LATERAL MOTIONS IN BEAM SEAS OF LONG WAVELENGTH

Specific consideration of beam seas of long wavelength yields considerable insight into the ship lateral motion problem. This is important from both a theoretical and a practical viewpoint since

a. classical treatment of ship lateral motions (see, for example, Chapter IX of Reference 11) generally concentrates on rolling in beam seas;

b. for ships of moderate to high metacentric height, rolling is greatest in beam seas.

Denote by F_{Ij} and H_j the total wave incident and diffraction forces, respecively, i.e. the itegrals over ship length of the sectional forces. Now, in beam seas, equations (84), (85) and (91) become

$$f_2 = -ik_w g A_x \tag{92}$$

$$f_4 = ik_w g M_x \tag{93}$$

$$h_j = -\frac{\omega}{\rho}(b_{2j} + i\omega a_{2j}) \tag{94}$$

since $\beta_s = 90^o$ and $\omega_w = \omega$.

Substitution of (92) to (94) into (24) and (25) and evaluation of the integrals yields

$$F_{I2} = -imgk_w a \tag{95}$$

$$H_2 = -\omega(B^H_{22} + i\omega A^H_{22})a \tag{96}$$

$$F_{I4} = ik_w mg\overline{GM}a \tag{97}$$

$$H_4 = -\omega(B^H_{24} + i\omega A^H_{24})a \tag{98}$$

$$F_{I6} = 0 \tag{99}$$

$$H_6 = -\omega[B^H_{26} + i\omega A^H_{26} + \frac{U}{i\omega}(B^H_{22} + i\omega A^H_{22})]a \tag{100}$$

Note that $\overline{GM}$ in equation (97) takes no account of internal free surfaces and that use of the CG as origin results in $F_{I6} = 0$.

Further, from equations (66) to (69) and (74) to (76), the following approximations hold:

$$F_2^F = (-\omega B_{22}^F - i\omega^2 A_{22}^F)a \tag{101}$$

$$F_2^C = -\omega B_{22}^C a \tag{102}$$

$$F_4^F = (-\omega B_{24}^F - i\omega^2 A_{24}^F)a \tag{103}$$

$$F_6^F = (-\omega B_{26}^F - i\omega^2 A_{26}^F)a \tag{104}$$

$$F_6^C = -\omega B_{26}^C a \tag{105}$$

Use will now be made of equations (95) to (105) to study lateral motions in beam seas of long wavelength, beginning with sway. In considering the sway equation, the roll and yaw coupling terms will be ignored, on the basis of the following reasoning.

The roll-to-sway coupling terms are $A_{24}\ddot{\eta}_4$ and $B_{24}\dot{\eta}_4$; note that in common with all wave-making damping terms, B_{24}^H, the dominant component of B_{24}, $\to 0$ as $\omega \to 0$. Now when waves are long relative to ship beam, both intuition and experience show that $\eta_4 = 0(\overline{\zeta})$, where

$$\overline{\zeta} = \frac{\frac{\omega^2 a}{w}}{g} \tag{106}$$

is wave slope. Hence the roll-to-sway coupling terms are both $0(\omega^4)$, and are negligible relative to F_2 which is $0(\omega^2)$.

The argument for neglect of yaw-to-sway coupling follows similar lines, since both intuition and experience suggest that yaw is much smaller than roll in beam seas.

Without the roll and yaw terms and with the asymptotic expressions for F_2, equation (1) becomes

$$[-\omega^2(A_{22} + m) + i\omega B_{22}]\eta_2 = F_{I2} + H_2 + F_2^F + F_2^C$$

$$= a[-imgk_w - \omega(B_{22}^H + i\omega A_{22}^H) - \omega(B_{22}^F + i\omega A_{22}^F) - \omega B_{22}^C]$$

$$= ia[-\omega^2(A_{22} + m) + i\omega B_{22}] \qquad (107)$$

$$\therefore \eta_2 = ia \qquad (108a)$$

Thus, sway amplitude equals wave amplitude and sway phase leads wave phase by 90^o.

Note that the approximations (95) to (105) were derived by neglecting the exponential decay of the wave forcing functions with depth (equation (80)). If this effect is included, however, by simply multiplying the right hand side of equation (107) by $\exp(-k_w C_M T)$, where T is draft and C_M midship sectional area coefficient, the resulting solution for η_2 is

$$\eta_2 = ia \exp(-k_w C_M T) \qquad (108b)$$

which is valid over a wider range of wavelengths than (108a).

Figure 4 demonstrates that equation (108b) gives a very good approximation of sway response, especially at low wave frequencies. The data plotted apply to a frigate at cruise speed in beam seas. The solid line is the result of solving the full equations of motion, while the dashed line is equation (108b). The validity of neglecting coupling of roll and yaw into sway is clearly demonstrated.

Consider next roll and ignore yaw coupling. From equation (2) with the asymptotic value (108) for η_2,

$$[-\omega^2(A_{44} + I_4) + i\omega B_{44} + C_{44}]\eta_4$$

$$= F_{I4} + H_4 + F_4^F - ia(-\omega^2 A_{24} + i\omega B_{24})$$

$$= a[ik_w mg\overline{GM} - \omega(B_{24}^H + i\omega A_{24}^H) - \omega(B_{24}^F + i\omega A_{24}^F) + \omega(B_{24} + i\omega A_{24})]$$

$$= ik_w amg\overline{GM} = iC_{44}\overline{\zeta} \tag{109}$$

Thus, sway coupling cancels both the wave diffraction moment and the foil exciting moment, and the result is the classical uncoupled rolling equation. Further, as $\omega \to 0$,

$$\eta_4 \approx i\overline{\zeta} \tag{110}$$

Thus, roll amplitude equals wave slope and roll phase leads wave phase by 90^o.

Consider finally the yaw equation. From equation (3) with η_2 given by (108),

$$[-\omega^2(A_{66} + I_6) + i\omega B_{66}]\eta_6 + [-\omega^2 A_{64} + i\omega B_{64}]\eta_4$$

$$= H_6 + F_6^F + F_6^C - ia(-\omega^2 A_{62} + i\omega B_{62})$$

$$= a\{-\omega[B_{26}^H + i\omega A_{26}^H + \frac{U}{i\omega}(B_{22}^H + i\omega A_{22}^H)] - \omega B_{26}^F - i\omega^2 A_{26}^F - \omega B_{26}^C$$

$$-i[-\omega^2 A_{26} + UB_{22}^H + i\omega(B_{26} + UA_{22}^H)]\}$$

$$= 0 \tag{111}$$

Thus, sway-to-yaw coupling cancels all the yaw exciting moments, and yaw results entirely from roll-to-yaw coupling:

$$\eta_6 = \left[\frac{\omega^2 A_{64} - i\omega B_{64}}{-\omega^2 (A_{66} + I_6) + i\omega B_{66}}\right]\eta_4 \qquad (112)$$

Since the denominator in equation (112) is always much greater in absolute value than the numerator and $\eta_4 = 0(\zeta)$, η_6 is very small.

In summary, then, the foregoing analysis illustrates the following points regarding lateral motions in beam seas of long wavelength:

1. Coupling of roll and yaw into sway is of little significance. Sway amplitude approaches wave amplitude and sway phase leads wave phase by 90^o.

2. Sway coupling into roll cancels the wave diffraction and foil exciting moments, and the roll equation reduces to the classical roll equation (109) in which only the wave incident moment appears on the right hand side. As wave frequency approaches zero, roll approaches wave slope and roll phase leads wave phase by 90^o.

3. Sway coupling into yaw cancels the yaw exciting moment, and yaw results entirely from roll-to-yaw coupling. Yaw is consequently virtually negligible.

4. The derivation of equation (109) shows very clearly the necessity of rigor when including the foil terms; A^F_{24}, B^F_{24} and F^F_4 must all be included to avoid erroneous results at low wave frequencies.

It is again emphasized that the above considerations apply only to beam seas of long wavelength. In particular, although the classical roll equation provides a good approximation for this case, it is wrong to assume that this will be true at other headings to the sea; only in beam seas where wave frequency equals frequency of encounter does the cancellation leading to equations (109) and (112) take place.

8. ROLL DAMPING

Good estimates of roll damping are essential for solving the roll prediction problem, particularly in beam seas where for long wavelengths equation (109) demonstrates that rolling dynamics reduce to a simple second order system. It is instructive to re-write this equation in the conventional form[12]:

$$\eta_4 = \left[\frac{\omega_o^2}{\omega_o^2 - \omega^2 + 2in\omega_o\omega}\right]\bar{\zeta} \tag{113}$$

where

$$\omega_o = \left(\frac{C_{44}}{A_{44} + I_4}\right)^{1/2} \tag{114}$$

is roll natural frequency, and

$$n = \frac{B_{44}}{2\omega_o(A_{44} + I_4)} = \frac{\omega_o B_{44}}{2C_{44}} \tag{115}$$

is roll decay coefficient. At resonance ($\omega = \omega_o$), equation (113) gives

$$\frac{\eta_4}{\bar{\zeta}} = \frac{1}{2n} \tag{116}$$

which illustrates the importance of an accurate estimate of n, as this parameter determines peak response in beam seas.

That the present theory does give reasonable estimates of roll damping is demonstrated in Figures 5 and 6, where theoretical predictions of n are compared with experimental values for two different warship hull forms of frigate size. The data in Figure 5 were obtained from calm water experiments with a 1:20.8-scale self-propelled model of the guided missile frigate, FFG-7[13], while the data in Figure 6 were measured during full scale forced rolling trials[12] of a Royal Navy frigate. Particulars on the hull forms are given in the references.

In Figure 5, n is plotted against initial angle of roll for speeds of 0, 5, 10 and 15 knots. The measurements were obtained by inclining the model to an initial roll angle, then releasing it and measuring the resulting roll decay characteristics. A large number of measurements were taken, and the resulting scatter gives a good idea of the experimental variability. Theory is in good agreement with the measurements at all four speeds shown. Especially noteworthy is the fact that the rapid increase in damping with increasing speed is well predicted. For the FFG-7, by far the greatest portion of this damping at non-zero speed results from the large spade rudder mounted directly behind the propeller. In making the theoretical estimates, the effects of propeller slipstream were accounted for using the data presented in Reference 14.

The ship of Figure 6 is equipped with fin stabilizers, which were employed in the trials to build up large roll angles which were then allowed to decay naturally with the fins locked in the mean position. The resulting measurements of n are plotted against speed, together with the theoretical estimates. Again, agreement between theory and experiment is good.

The importance of including dynamic lift on appendages in predicting roll damping has already been mentioned. Figures 7 and 8 illustrate this point, giving a theoretical breakdown of B_{44} between viscous (B^V_{44}) and non-viscous ($B^H_{44} + B^F_{44}$) contributions. Recall from Section 2 to 5 that B^V_{44}, B^F_{44} and B^H_{44} are, respectively, the viscous, foil dynamic lift, and hull wave-making components of roll damping. All damping components are evaluated at the roll natural frequency. Initial roll amplitude is 5^o and the speed range is 0-25 knots. Figure 7 is representative of a frigate with twin rudders, one pair of fins and one set of bilge keels, while Figure 8 applies to a destroyer with a single rudder, no fins and a relatively longer pair of bilge keels.

The dominance of the non-viscous contribution at cruise speeds is readily apparent. Further, for both ships the non-viscous portion results almost entirely from dynamic lift. Figure 9 illustrates this point for the destroyer, giving a plot against freqeuncy of B^F_{44}, B^H_{44} and B^V_{44} at a speed of 20 knots. At the roll natural frequency, to which the data in Figure 8 apply, wave-making damping is relatively low.

Figures 7 to 9 clearly show that it is essential to include dynamic lift in theoretical estimates of roll damping. Without this effect, damping will be significantly under-predicted at even moderate speeds.

9. COMPARISON OF THEORY WITH EXPERIMENT

Experimental data for comparison with theory have been obtained from three sources: regular wave tests[2] with a fully-appended self-propelled frigate model at the seakeeping basin of the David Taylor Naval Ship Research and Development Center (DTNSRDC), sea trials[15] of the oceanographic research ship CFAV QUEST, and sea trials[12] of the same ship for which roll damping data are given in Figure 6. Only roll data are presented, since measurements of sway and yaw are virtually non-existent.

Figures 10 to 14 present extensive experimental data for the frigate model tested at DTNSRDC. This was a comprehensive experimental program in which metacentric height, bilge keel configuration, heading and forward speed were systematically varied. Two different bilge keels were used (designated BK_1 and BK_3) and three metacentric heights (GM_1, GM_2 and GM_3). Some details are given below.

Length between perpendiculars	18.182 ft
Beam	2.156 ft
Draft	.716 ft
Block coefficient	.485
Prismatic coefficient	.604

Metacentric height designation	% of beam
GM_1	12.1
GM_2	9.0
GM_3	6.1

Bilge keel designation	Area in % of wetted area	Length in % of LBP
BK_1	2.34	29.6
BK_3	1.00	17.0

Figures 10 and 11 show the effect on roll response of varying sea direction at low and high Froude numbers, respectively. Figures 12 and 13 show the effect of varying metacentric height and bilge keel configuration at low Froude number in bow seas and high Froude number in beam seas. Finally, Figure 14 presents data showing the influence of metacentric height on roll response in quartering seas at low Froude number.

Agreement between theory and experiment is generally good and sometimes near-perfect. The following points are especially worthy of mention:

1. The considerable variation in roll response with heading to the sea is reasonably well predicted, both at low and high speed.

2. Predictions of peak response are generally good, indicating good estimation of roll damping.

3. Theory correctly predicts a substantial reduction in roll response as speed increases. This decrease is mainly due to the twin rudders, which contribute significantly to roll damping at high speed.

4. The dramatic increase in roll response in quartering seas as metacentric height is reduced is very well predicted. This is of considerable practical importance, since the GM_3 case is representative of the metacentric height/beam ratio at which frigates and destroyers commonly operate.

Figures 15 and 16 present sea trials data for CFAV QUEST, for which the leading particulars are[15]:

Displacement during trials	2255 tons
Length between perpendiculars	234 ft
Beam	42 ft
Draft	16 ft

Figure 15 compares computed and measured roll response at 0 and 10 knots. The experimental points were obtained from roll and wave spectra measured during the trials, simultaneously in the case of zero speed. Agreement between theory and measurement is good, particularly since the measurements come from full scale sea trials with attendant uncertainties in wave direction and spectral measurement. Again

the decrease in peak response with increasing speed is correctly predicted.

Figure 16 shows that when the theoretical beam sea roll responses given in Figure 15 are applied to the wave spectra measured during the trials, a good estimate of root mean square roll angle is obtained. Data are also given in Figure 16 for the bow and quartering sea directions, and again reasonable agreement is demonstrated, even though the theoretical calculation has been performed for a long-crested sea.

Finally, Figure 17 presents beam sea roll response data extracted from Reference 13. Some ship particulars are listed below; note the presence of a single pair of fin stabilizers, which were locked in the mean position during the trials.

Displacement during trails	2500 tons
Length between perpendiculars	350 ft
Beam	43 ft
Draft	12 ft
Stabilizer fin area	28 ft^2

Results are given in Figure 17 for three speeds (12, 16 and 20 knots). As for the QUEST results in Figure 15, the experimental points were obtained from roll and wave spectra measured during the trials. Three sets of measurements were obtained at 16 and 20 knots, and two at 12 knots. Agreement between theory and experiment is good, particularly at the two higher speeds.

10. CONCLUSION

A theoretical model has been developed for the prediction of ship lateral motions in oblique seas. The asymptotic behaviour of this model in waves that are long relative to ship beam has been examined, with particular emphasis on the classical problem of rolling in beam seas. It has been demonstrated that the model gives reasonable estimates of roll damping, and the importance of including dynamic lift in theoretical predictions of roll damping has been emphasized. Fairly extensive comparisons of predicted and measured roll response show generally good agreement at all headings to the sea, suggesting that the theory yields predictions of sufficient accuracy for preliminary design purposes.

REFERENCES

1. Meyers, W. G., Sheridan, D. J. and Salvesen, N.: "Manual NSRDC Ship-Motion and Sea-Load Computer Program". *NSRDC Report* 3376, February 1975.

2. Baitis, A. E. and Wermter, R.: "A Summary of Oblique Sea Experiments Conducted at the Naval Ship Research and Development Center". 13th International Towing Tank Conference, 1972.

3. Raff, A. I.: "Program SCORES - Ship Structural Response in Waves". Ship Structure Committee Report No. SSC 230, 1972.

4. Schmitke, R. T.: "Predictions of Wave-Induced Motions for Hullborne Hydrofoils". J. Hydronautics, 1977.

5. Salvesen, N., Tuck, E. O., and Faltinsen, O.: "Ship Motions and Sea Loads". Trans., SNAME, Vol. 78, 1970.

6. Kato, H.: "Effect of Bilge Keels on the Rolling of Ships". Memories of the Defence Academy, Japan, Vol. 4, 1966.

7. Tanaka, N.: "A Study on the Bilge Keels (Part 4 - On the Eddy-Making Resistance to the Rolling of a Ship Hull)". Society of Naval Architects of Japan, Vol. 109, 1960.

8. Kato, H.: "On the Frictional Resistance to the Roll of Ships". Society of Naval Architects of Japan, Vol. 102, 1958.

9. Hoerner, S. F.: "Fluid Dynamic Drag". Published by the Author, 1958.

10. Drummond, T. G., Mackay, M., and Schmitke, R. T.: "Wave Impacts on Hydrofoil Ships and Structural Implications". Eleventh Symposium on Naval Hydrodynamics, London, 1976.

11. Comstock, J. P. (Ed): "Principles of Naval Architecture". SNAME, 1967.

12. Conolly, J. E.: "Rolling and Its Stabilization by Active Fins". RINA Trans., Vol. 111 (1969).

13. Jones, H. D. and Cox, C. G.: "Roll Stabilization Investigation for the Guided Missile Frigate (FFG-7)". DTNSRDC Ship Performance Department Report SPD-495-18, July 1976.

14. Boswell, R. J.: "The Distribution of Force and Torque on the Rudder of a Surface Warship". AEW Report 9/74, February, 1974.

15. Miles, M.: "Tuning and Evaluation of Anti-Roll Tanks on CFAV QUEST". NRC Report LTR-SH-122, January 1972.

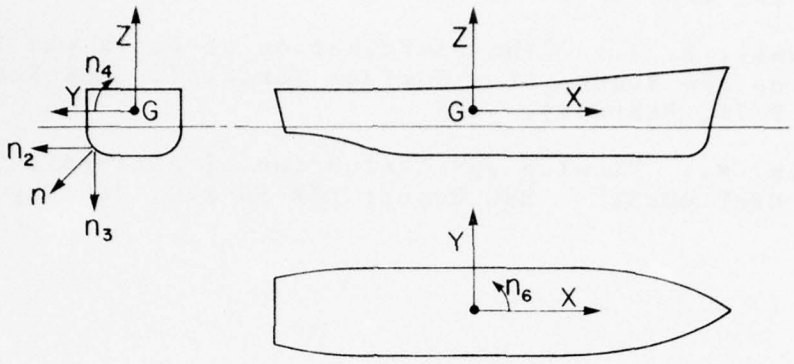

FIG. 1 , AXIS SYSTEM

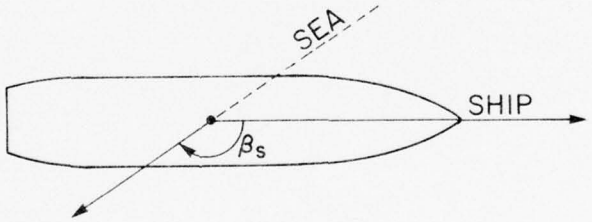

FIG. 2 , DEFINITION OF SEA DIRECTION

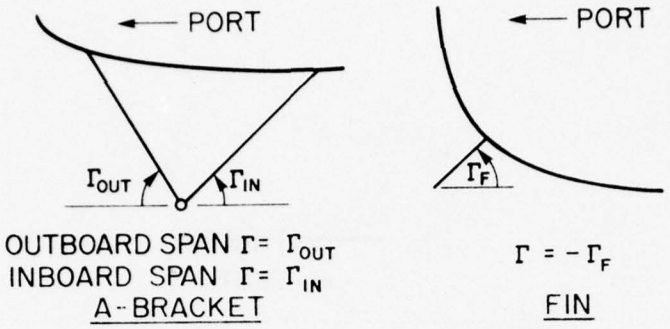

FIG. 3, DIHEDRAL ANGLE CONVENTION

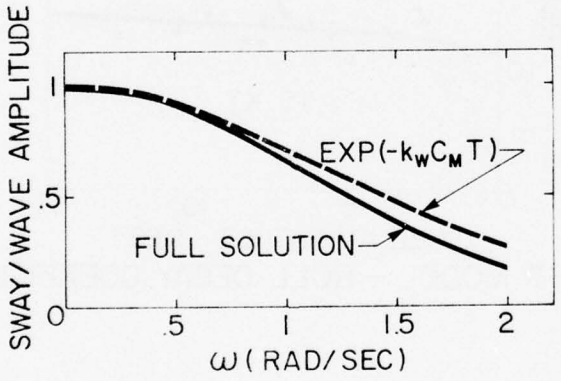

FIG. 4, FRIGATE SWAY RESPONSE IN BEAM SEAS

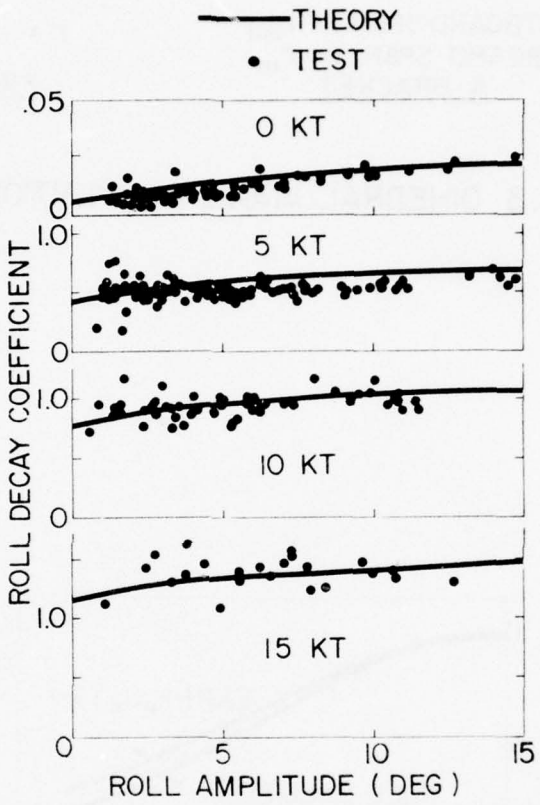

FIG.5, FFG-7 MODEL – ROLL DECAY COEFFICIENT

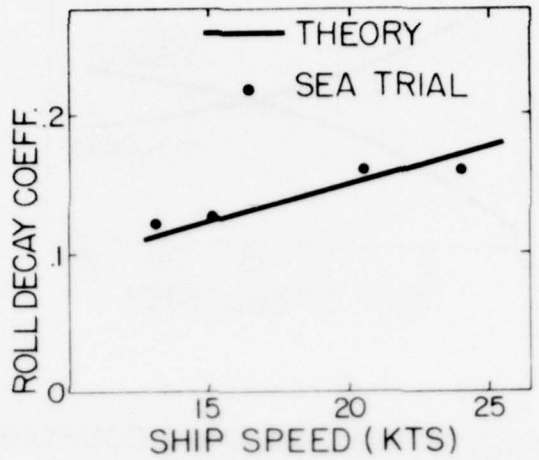

FIG. 6, FRIGATE ROLL DECAY COEFFICIENT

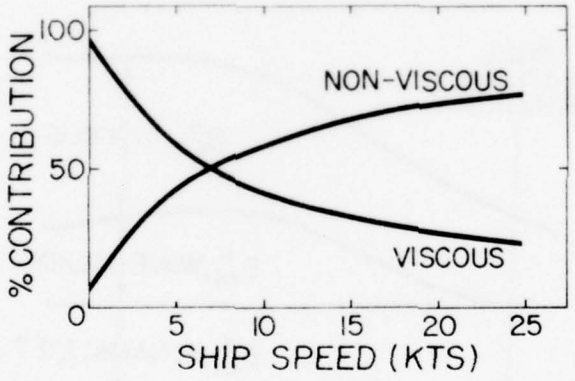

FIG. 7, FRIGATE ROLL DAMPING COMPONENTS
WITH TWIN RUDDERS, ONE PAIR OF FINS

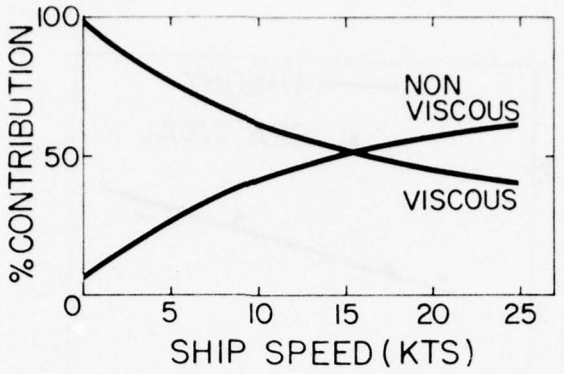

FIG.8, DESTROYER ROLL DAMPING COMPONENTS WITH SINGLE RUDDER, NO FINS

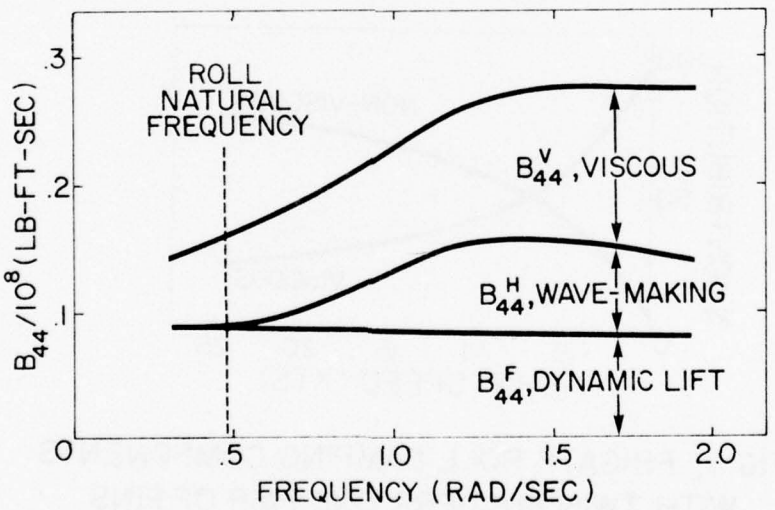

FIG.9, DESTROYER ROLL DAMPING COMPONENTS AT 20 KNOTS

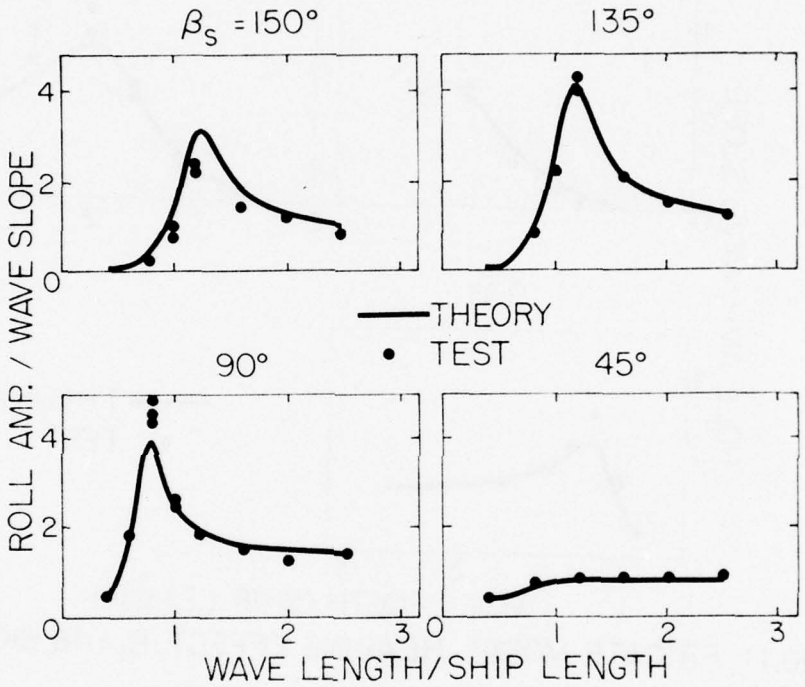

FIG. 10, FRIGATE MODEL, HEADING EFFECT, $F_n = .15$, $BK_1\,GM_1$

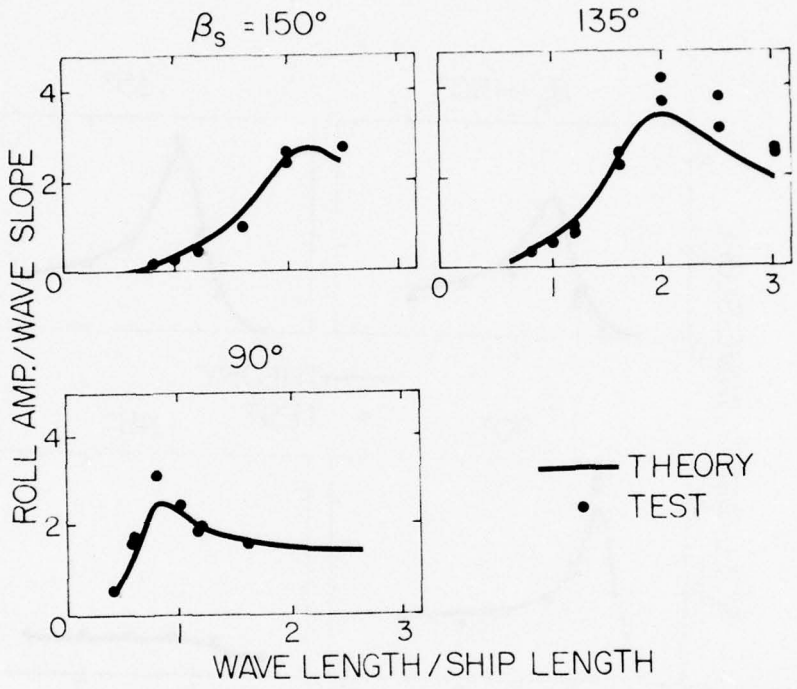

FIG. 11, FRIGATE MODEL, HEADING EFFECT, $F_n = .46$, $BK_1 GM_1$

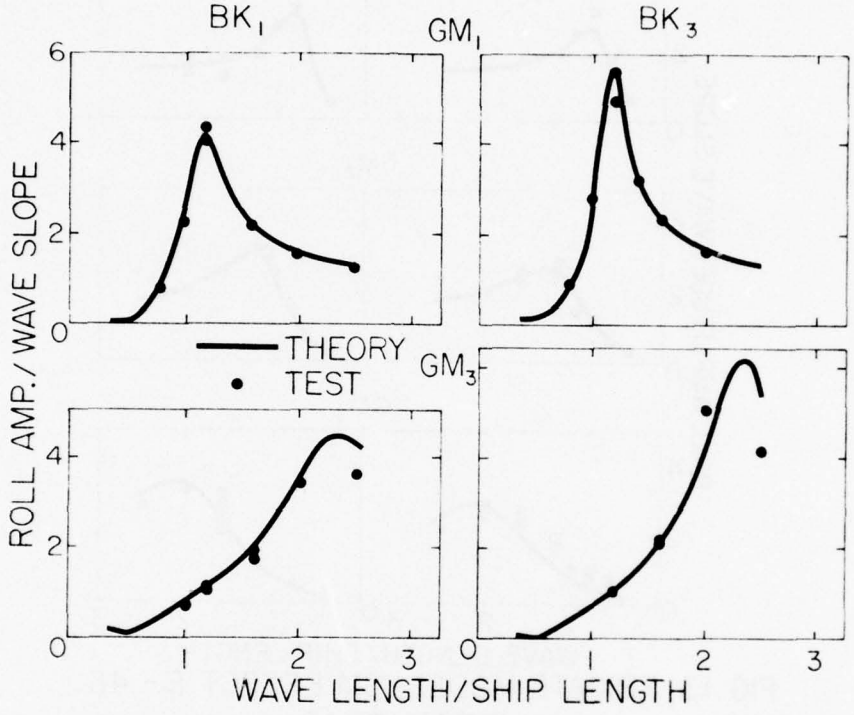

FIG.12, FRIGATE MODEL, GM EFFECT, F_n = .15, BOW SEAS

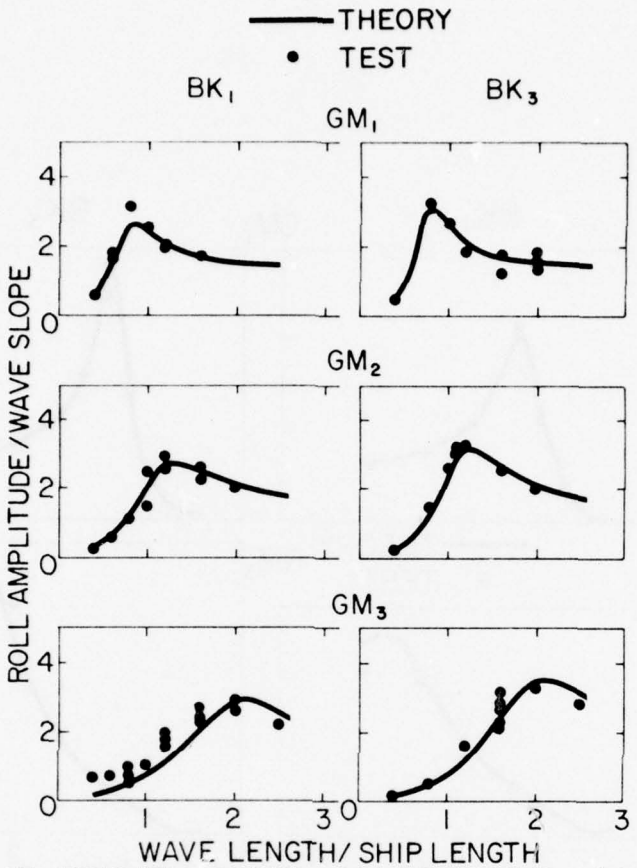

FIG. 13, FRIGATE MODEL–GM EFFECT $F_n = .46$
BEAM SEAS

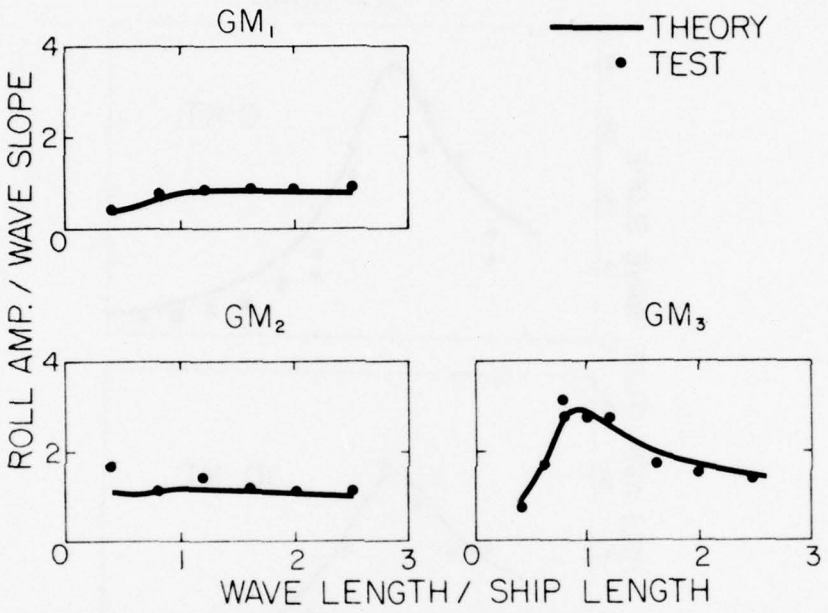

FIG. 14, FRIGATE MODEL, GM EFFECT, F_n = .15
QUARTERING SEAS

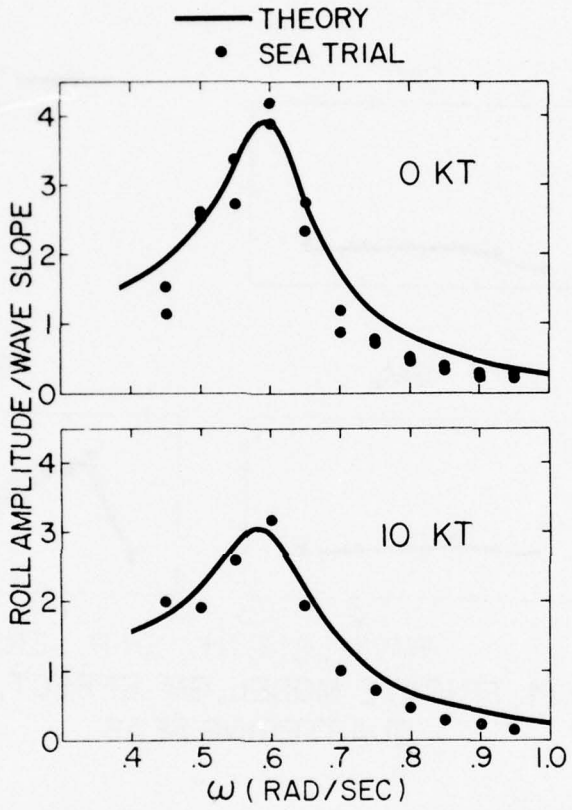

FIG. 15, CFAV QUEST – ROLL RESPOSE IN BEAM SEAS

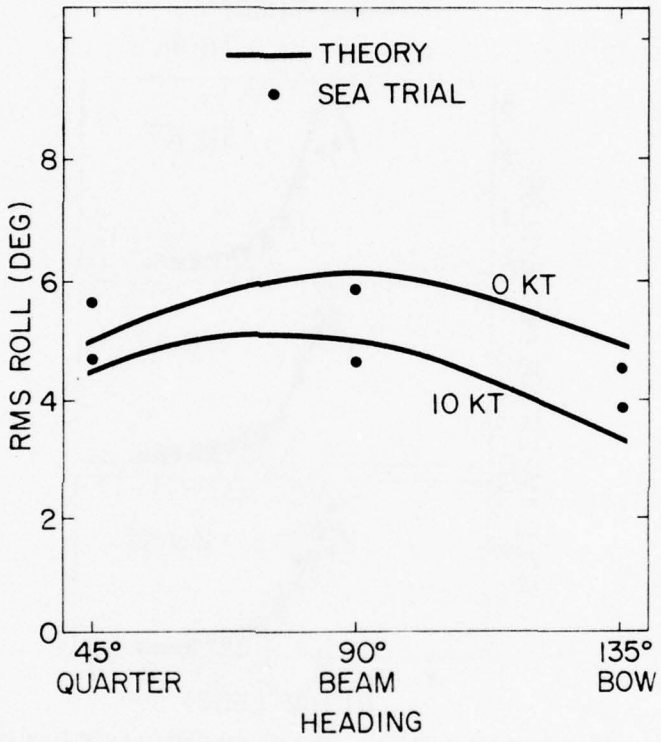

FIG. 16, CFAV QUEST – RMS ROLL VS HEADING

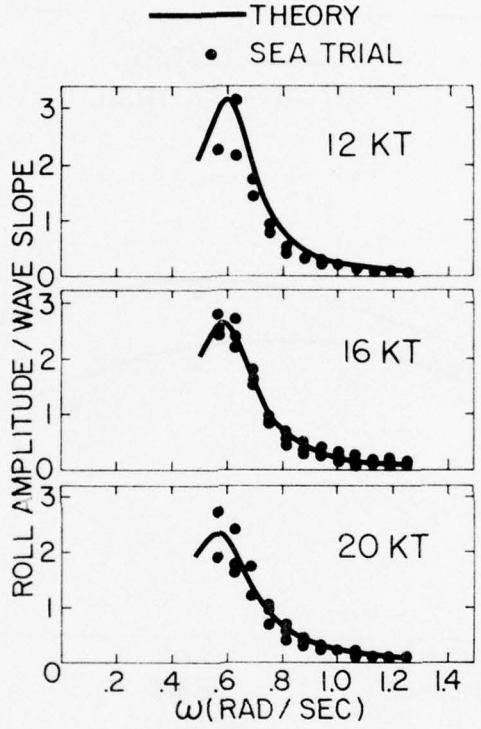

FIG. 17, FRIGATE ROLL RESPONSE IN BEAM SEAS

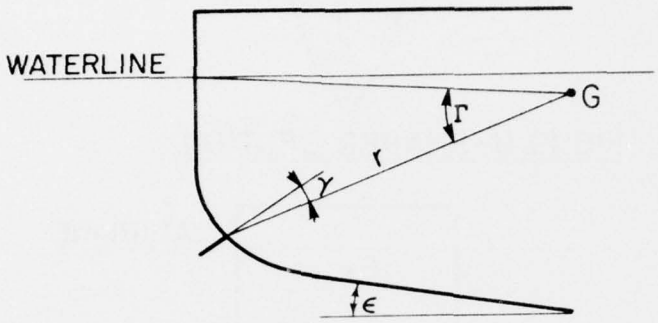

$$F_r = \frac{B}{2} \tan \epsilon$$

FIG. 18 BILGE KEEL PARAMETERS

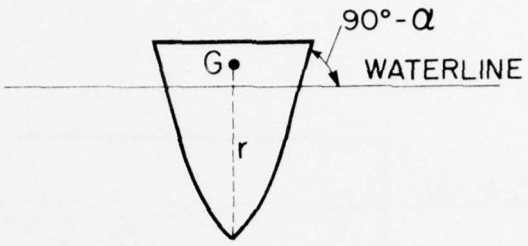

FIG. 19, U-SHAPED SECTION

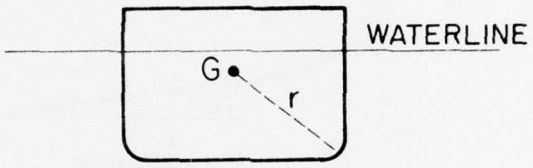

FIG. 20, FULL SECTION

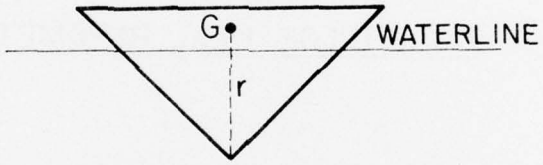

FIG. 21, TRIANGULAR SECTION

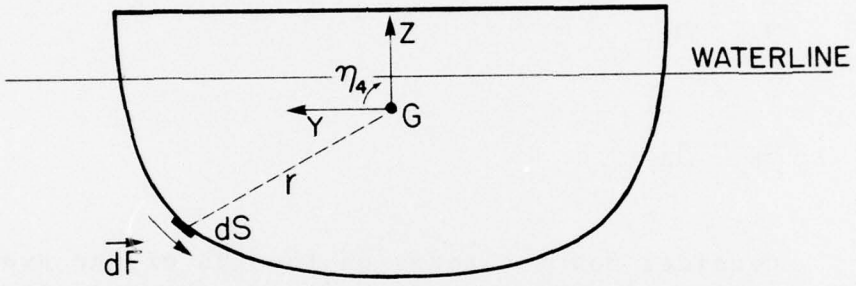

FIG. 22, HULL SECTION SHOWING dS AND $\vec{dF}$

APPENDIX A

ADDED MASS AND DAMPING COEFFICIENTS IN STABILITY AXES

The coefficients given in Reference 4 apply to translating earth axes. The translation to stability axes is

$$\dot{\eta}_2 \rightarrow \dot{\eta}_2 + U\eta_6 = \dot{\eta}_2 + \frac{U}{i\omega}\dot{\eta}_6 = \dot{\eta}_2 - \frac{U}{\omega^2}\ddot{\eta}_6$$

$$\eta_4 \rightarrow \eta_4$$

$$\eta_6 \rightarrow \eta_6$$

Consider now the terms on the LHS of the sway, roll, and yaw equations in Reference 4. Ignore the end-effect terms and perform the above axis transformation.

Sway:

$$[\int_L a_{22}d\xi](\ddot{\eta}_2 + U\dot{\eta}_6) + [\int_L b_{22}d\xi](\dot{\eta}_2 - \frac{U}{\omega^2}\ddot{\eta}_6) + A_{24}\ddot{\eta}_4 + B_{24}\dot{\eta}_4$$

$$+ [\int_L a_{22}\xi d\xi + \frac{U}{\omega^2}\int_L b_{22}d\xi]\ddot{\eta}_6 + [\int_L b_{22}\xi d\xi - U\int_L a_{22}d\xi]\dot{\eta}_6$$

$$= [\int_L a_{22}d\xi]\ddot{\eta}_2 + [\int_L b_{22}d\xi]\dot{\eta}_2 + A_{24}\ddot{\eta}_4 + B_{24}\dot{\eta}_4 + [\int_L a_{22}\xi d\xi]\ddot{\eta}_6$$

$$+ [\int_L b_{22}d\xi]\dot{\eta}_6$$

Roll:

$$[\int_L a_{24} d\xi](\ddot{\eta}_2 + U\dot{\eta}_6) + [\int_L b_{24} d\xi](\dot{\eta}_2 - \frac{U}{\omega^2}\ddot{\eta}_6) + A_{44}\ddot{\eta}_4 + B_{44}\dot{\eta}_4$$

$$+ [\int_L a_{24}\xi d\xi + \frac{U}{\omega^2}\int_L b_{24} d\xi]\ddot{\eta}_6 + [\int_L b_{24}\xi d\xi - U\int_L a_{24} d\xi]\dot{\eta}_6$$

$$= [\int_L a_{24} d\xi]\ddot{\eta}_2 + [\int_L b_{24} d\xi]\dot{\eta}_2 + A_{44}\ddot{\eta}_4 + B_{44}\dot{\eta}_4 + [\int_L a_{24}\xi d\xi]\ddot{\eta}_6$$

$$+ [\int_L b_{24}\xi d\xi]\dot{\eta}_6$$

Yaw:

$$[\int_L a_{22}\xi d\xi - \frac{U}{\omega^2}\int_L b_{22} d\xi](\ddot{\eta}_2 + U\dot{\eta}_6)$$

$$+ [\int_L b_{22}\xi d\xi + U\int_L a_{22} d\xi](\dot{\eta}_2 - \frac{U}{\omega^2}\ddot{\eta}_6)$$

$$+ A_{64}\ddot{\eta}_4 + B_{64}\dot{\eta}_4 + [\int_L a_{22}\xi^2 d\xi + \frac{U^2}{\omega^2}\int_L a_{22} d\xi]\ddot{\eta}_6$$

$$+ [\int_L b_{22}\xi^2 d\xi + \frac{U^2}{\omega^2}\int_L b_{22} d\xi]\dot{\eta}_6$$

$$= [\int_L a_{22}\xi d\xi - \frac{U}{\omega^2}\int_L b_{22} d\xi]\ddot{\eta}_2 + [\int_L b_{22}\xi d\xi + U\int_L a_{22} d\xi]\dot{\eta}_2$$

$$+ A_{64}\ddot{\eta}_4 + B_{64}\dot{\eta}_4 + [\int_L a_{22}\xi^2 d\xi]\ddot{\eta}_6 + [\int_L b_{22}\xi^2 d\xi]\dot{\eta}_6$$

APPENDIX B

BILGE KEEL ROLL DAMPING

Equations for the calculation of the coefficients C_o, C_a m C_k, C_n, Ⓑ, F, and α in equation (36) are given in this Appendix.

The coefficient F depends upon r, $\hat{\eta}_4$, T, b_k and Γ, the angle between the waterline, CG and bilge keel root (Figure 18):

$$F = \frac{3.13 r \hat{\eta}_4}{T\sqrt{g b_k}} \Gamma^{1.7}$$

The index α is also a function of r, b_k and Γ:

$$\alpha = .6 - 2.03\exp(-25\xi)$$

where

$$\xi = \frac{b_k}{r\Gamma^{.75}}$$

The coefficient Ⓑ depends upon the length of girth from bilge keel root to waterline s, beam B, height of CG above keel $\overline{KG}$, draft d and rise of floor F_r:

$$Ⓑ = \cos\gamma + \frac{s}{2b_k r}[q + p_o - (p_o - p_1) f(\lambda)]$$

where γ is the angle made by the plane of the bilge keel with the straight line passing through the CG and the bilge keel root.

$$q = [\frac{B}{2}\tan(\frac{\pi}{4} - \frac{\varepsilon}{2}) + F_r - \overline{KG}]\sin(\frac{\pi}{4} + \frac{\varepsilon}{2})$$

$$\varepsilon = \tan^{-1}\left[\frac{2F_r}{B}\right]$$

$$p_o = \overline{KG} - \frac{d}{3} - \frac{2}{3}F_r$$

$$p_1 = .88\{\overline{KG} - d - .54[\frac{B}{2} - (d - F_r)\tan(\frac{\pi}{4} + \frac{\varepsilon}{2})]\}$$

$$f(\lambda) = \frac{1.34\sin\frac{\pi\lambda}{3.6}}{1 + .162\sin[\frac{\pi}{1.8}(\lambda - .9)]}$$

$$\lambda = \frac{R}{d - \frac{F_r}{B}(B - 2R)}$$

C_n is the normal pressure coefficient for a rectangular plate moving with a uniform velocity in the direction perpendicular to its plane:

$$C_n = \begin{cases} 1.98\exp(-11b_k/\ell), & b_k/\ell < .048 \\ 1.17, & b_k/\ell \geq .048 \end{cases}$$

The coefficient C_k depends upon ship form and in particular upon R, the bilge radius:

$$C_k = 1 + 3.5e^{-9k}$$

$$k = \frac{R(1 + \frac{F_r}{B})^2}{\sqrt{\frac{B}{2KG}}}$$

C_a is a function of the rolling Reynolds number R_N, given by

$$R_N = \frac{8b_k r\hat{\eta}_4}{T\nu}$$

where ν is kinematic viscosity.

$$C_a = \begin{cases} 1, & R_N \geq 10^3 \\ 1.95 - .251\log R_N + .2\sin[\frac{\pi}{.54}(\log R_N - 2.19)], & R_N < 10^3 \end{cases}$$

Finally, the coefficient C_o depends upon Γ and also serves to scale the overall equation:

$$C_o = 14.1 + 37.3\Gamma^3$$

APPENDIX C

EDDY-MAKING ROLL DAMPING

Empirical equations based on Tanaka's results[7] are presented below for evaluation of C, the eddy-making drag coefficient.

Consider first V or U-shaped sections, Figure 19, as are encountered in the foremost part of a ship. Tanaka has obtained the following empirical equation.

$$C = T_1\left(\frac{B}{\overline{KG}}\right) T_2\left(\alpha, \frac{R_e}{d}\right) \exp\left(-u\frac{R_e}{d}\right) \qquad \text{(C-1)}$$

where α is the angle of inclination of the ship side at the water line (Figure 19), R_e is the effective radius at the keel and u is a function of $\hat{\eta}_4$. T_1 and T_2 are tabulated in Tables 1 and 2 respectively. Empirical equations for R_e and u, obtained by fitting least squares quadratics to Tanaka's data, are given below.

$$u = 14.1 - 46.7\hat{\eta}_4 + 61.7\hat{\eta}_4^2$$

$$R_e = \begin{cases} \frac{B}{2}\left[4.12 - 3.69\frac{\overline{KG}}{B} + .823\left(\frac{\overline{KG}}{B}\right)^2\right], & \frac{\overline{KG}}{B} < 2.1 \\ 0, & \frac{\overline{KG}}{B} \geq 2.1 \end{cases} \qquad \text{(C-2)}$$

Consider now very full, almost rectangular, sections, as shown in Figure 20. Equations (C-1) and (C-2) are used with r the distance from the CG to the bilge, R_e the bilge radius and $T_2 = 1$.

Finally, consider triangular sections, Figure 21, as are found farthest aft in cruiser stern ships. For these sections C is a function of $B/\overline{KG}$ alone. The following quadratic has been fitted to Tanaka's data.

$$C = .438 - .449\left(\frac{B}{\overline{KG}}\right) + .236\left(\frac{B}{\overline{KG}}\right)^2$$

B_E is calculated by a strip method, with each section either placed in one of the above three categories or neglected. An example of a section whose eddy-making effect is negligible is a destroyer mid-section with extremely rounded bilges and no skeg.

TABLE I - T_1 vs. $B/\overline{KG}$

$B/\overline{KG}$	T_1
0.0	.50
0.25	.61
0.5	.62
1.0	.61
1.5	.53
2.0	.40
2.5	.35
3.0	.32
3.5	.29
4.0	.26

TABLE II - T_2 vs. α and R_e/d

α(deg)	$R_e/d = 0$	.0571	.1142	.1713
0	1.00	1.00	1.00	1.00
5	.86	.75	.74	.70
10	.77	.67	.72	.72
20	.68	.75	.89	1.20
30	.65	.92	1.34	1.94

APPENDIX D

HULL FRICTION ROLL DAMPING

Consider an element of hull surface dS, Figure 22. The skin friction drag force $\vec{dF}$ acting on dS as a result of the rolling velocity $\dot{\eta}_4$ is given by

$$\vec{dF} = \frac{1}{2}\rho r(yn_2 + zn_3)\dot{\eta}_4|\dot{\eta}_4|C_{DF}dS(n_3\vec{j} - n_2\vec{k})$$

where C_{DF} is the skin friction drag coefficient, $\vec{j}$ and $\vec{k}$ are unit vectors along the y and z axes, and

$$r = \sqrt{y^2 + z^2}$$

is the distance from dS to the CG.

$\vec{dF}$ exerts a torque about the rolling axis given by

$$dT = -\frac{1}{2}\rho r(yn_2 + zn_3)^2\dot{\eta}_4|\dot{\eta}_4|C_{DF}dS$$

The energy dissipated by dT during one roll cycle is

$$dE = \frac{4}{3}\rho r(yn_2 + zn_3)^2\omega^2\hat{\eta}_4^3C_{DF}dS$$

Hence, upon integrating dS over the hull by a strip method, equation (43) is obtained.

APPENDIX E

ROLL-RESTORING MOMENT

Consider an element of hull area dA, located at (x, y, z). When the ship rolls through a small angle η_4, the hydrostatic force acting on dA increases by

$$df = -\rho g \eta_4 y dA$$

df acts normal to the hull, with y and z components:

$$df_y = -n_2 df$$

$$df_z = -n_3 df$$

The rolling moment exerted by df is

$$dK = y df_z - z df_y = (-yn_3 + zn_2) df$$

$$= -\rho g \eta_4 y(-yn_3 + zn_2) dA$$

$$= -\rho g \eta_4 y(-yn_3 + zn_2) dx d\ell$$

Integration over the hull gives the total roll-restoring moment

$$K = -\rho g \eta_4 \int_L M_x dx$$

where M_x is the sectional contribution to the roll-restoring moment:

$$M_x = \int_{C_x} (-yn_3 + zn_2) y d\ell$$

UNCLASSIFIED

Security Classification

DOCUMENT CONTROL DATA - R & D

(Security classification of title, body of abstract and indexing annotation must be entered when the overall document is classified)

1. ORIGINATING ACTIVITY

Defence Research Establishment Atlantic

2a. DOCUMENT SECURITY CLASSIFICATION
Unclassified

2b. GROUP

3. DOCUMENT TITLE

(6) PREDICTION OF SHIP ROLL, SWAY AND YAW MOTIONS IN OBLIQUE WAVES

4. DESCRIPTIVE NOTES (Type of report and inclusive dates) DREA Report

5. AUTHOR(S) (Last name, first name, middle initial)

(10) R. T. Schmitke (11)

6. DOCUMENT DATE

Sep[illegible]77

7a. TOTAL NO. OF PAGES
67

7b. NO. OF REFS
15

8a. PROJECT OR GRANT NO.

~~23B~~

8b. CONTRACT NO.

9a. ORIGINATOR'S DOCUMENT NUMBER(S)

(14) DREA-774

DREA REPORT 774

9b. OTHER DOCUMENT NO.(S) (Any other numbers that may be assigned this document)

(12) 69 p.

10. DISTRIBUTION STATEMENT

11. SUPPLEMENTARY NOTES

12. SPONSORING ACTIVITY

DREA

13. ABSTRACT

A theoretical model is developed for the prediction of ship lateral motions in oblique seas. The asymptotic behaviour of this model in waves that are long relative to ship beam is examined, with particular emphasis on the classical problem of rolling in beam seas. The theoretical prediction of roll damping is discussed, and the importance of including dynamic lift on appendages is emphasized. Fairly extensive comparisons of predicted and measured roll response are made, with good agreement at all headings considered.

DSIS
78-078

403 761

KEY WORDS

ship motion theory
roll
sway
yaw
waves

INSTRUCTIONS

1. ORIGINATING ACTIVITY: Enter the name and address of the organization issuing the document.

2a. DOCUMENT SECURITY CLASSIFICATION: Enter the overall security classification of the document including special warning terms whenever applicable.

2b. GROUP: Enter security reclassification group number. The three groups are defined in Appendix 'M' of the DRB Security Regulations.

3. DOCUMENT TITLE: Enter the complete document title in all capital letters. Titles in all cases should be unclassified. If a sufficiently descriptive title cannot be selected without classification, show title classification with the usual one-capital-letter abbreviation in parentheses immediately following the title.

4. DESCRIPTIVE NOTES: Enter the category of document, e.g. technical report, technical note or technical letter. If appropriate, enter the type of document, e.g. interim, progress, summary, annual or final. Give the inclusive dates when a specific reporting period is covered.

5. AUTHOR(S): Enter the name(s) of author(s) as shown on or in the document. Enter last name, first name, middle initial. If military, show rank. The name of the principal author is an absolute minimum requirement.

6. DOCUMENT DATE: Enter the date (month, year) of Establishment approval for publication of the document.

7a. TOTAL NUMBER OF PAGES: The total page count should follow normal pagination procedures, i.e., enter the number of pages containing information.

7b. NUMBER OF REFERENCES: Enter the total number of references cited in the document.

8a. PROJECT OR GRANT NUMBER: If appropriate, enter the applicable research and development project or grant number under which the document was written.

8b. CONTRACT NUMBER: If appropriate, enter the applicable number under which the document was written.

9a. ORIGINATOR'S DOCUMENT NUMBER(S): Enter the official document number by which the document will be identified and controlled by the originating activity. This number must be unique to this document.

9b. OTHER DOCUMENT NUMBER(S): If the document has been assigned any other document numbers (either by the originator or by the sponsor), also enter this number(s).

10. DISTRIBUTION STATEMENT: Enter any limitations on further dissemination of the document, other than those imposed by security classification, using standard statements such as:

(1) "Qualified requesters may obtain copies of this document from their defence documentation center."

(2) "Announcement and dissemination of this document is not authorized without prior approval from originating activity."

11. SUPPLEMENTARY NOTES: Use for additional explanatory notes.

12. SPONSORING ACTIVITY: Enter the name of the departmental project office or laboratory sponsoring the research and development. Include address.

13. ABSTRACT: Enter an abstract giving a brief and factual summary of the document, even though it may also appear elsewhere in the body of the document itself. It is highly desirable that the abstract of classified documents be unclassified. Each paragraph of the abstract shall end with an indication of the security classification of the information in the paragraph (unless the document itself is unclassified) represented as (TS), (S), (C), (R), or (U).

The length of the abstract should be limited to 20 single-spaced standard typewritten lines; 7½ inches long.

14. KEY WORDS: Key words are technically meaningful terms or short phrases that characterize a document and could be helpful in cataloging the document. Key words should be selected so that no security classification is required. Identifiers, such as equipment model designation, trade name, military project code name, geographic location, may be used as key words but will be followed by an indication of technical context.